Spectrochimica Acta Vol 45B, No. 4/5, pp 481–491, 1990
Printed in Great Britain

0584–8547/90 $3.00+.00
Pergamon Press plc

Multi-component standard additions and partial least squares modelling—a multivariate calibration approach to the resolution of spectral interferences in graphite furnace atomic absorption spectrometry

D. C. BAXTER
Department of Analytical Chemistry, University of Umeå, S-901 87 Umeå, Sweden

and

J. ÖHMAN*
Umetri AB, Box 1456, S-901 24 Umeå, Sweden

(*Received* 1 *August* 1989; *in revised form* 22 *September* 1989)

Abstract—Spectral interferences in graphite furnace atomic absorption spectrometry (GFAAS) represent a considerable problem, often making the direct determination of certain elements in specific matrices impossible, particularly when continuum source background correction is employed. The possibilities to resolve such spectral interferences mathematically by applying multivariate calibration have been investigated. Resolution is achieved using multi-component standard additions (the so-called generalised standard addition method or GSAM) combined with partial least squares (PLS) modelling. This multivariate calibration method, PLS–GSAM, is described and its use illustrated by application to the GFAAS determination of gold in the presence of cobalt at the 242.8 nm wavelength, where severe spectral interference problems are observed using continuum source background correction. Two requirements for the successful application of PLS–GSAM are that the sample constituent causing the spectral interference is known and that its concentration can be increased by standard additions. It is shown that more accurate results are obtained by PLS–GSAM than by conventional (single-component) standard addition methods.

1. INTRODUCTION

IN THE field of analytical chemistry, graphite furnace atomic absorption spectrometry (GFAAS) is one of the instrumental methods that comes closest to fulfilling the requirements for a "fully selective detector" as defined by KAISER [1]. This enviable status results from the inherent high resolution achieved in AAS by the use of narrow line sources [2], and the introduction of background correction techniques permitting accurate, simultaneous compensation for most sample concomitant species covolatilised with the analyte during the atomisation/measurement step [3, 4].

At present, the most widely adopted background correction system employs a continuum source lamp [5] to quantify the non-specific absorbance. The major limitation of this approach—that the non-specific absorbance must be of an even, structureless and continuous nature over the spectral bandwidth isolated by the monochromator—was soon recognised and led to the development of the more efficient pulsed hollow cathode lamp (Smith–Hieftje) [4, 6] and Zeeman-effect background correction [3, 4, 7] techniques. However, even these may be susceptible to spectral interferences, i.e. give erroneous background correction under certain circumstances [4, 8–10].

When background correction errors occur, it is generally recommended to use alternative wavelengths, or to separate the element of interest from the interfering matrix components, but there are obvious disadvantages to both measures. Here, another possibility is examined, that of utilising multivariate calibration [11] to compensate for background correction errors. The method involves making multi-component standard additions (the generalised standard addition method or GSAM [12, 13]) to generate a calibration set and partial least squares (PLS [14–16]) modelling to describe the absorbance profiles obtained. After a brief presentation of the multivariate approach to resolving the spectral inteference problem, a

* Present address: National Swedish Laboratory for Agricultural Chemistry, Box 5097, S-900 05 Umeå, Sweden.

preliminary example illustrating the potential of the method is given. Specifically, gold is shown to be fairly accurately determined at the primary 242.8 nm resonance line by GFAAS using continuum source background correction in the presence of excess cobalt, the latter causing severe spectral interferences [17].

2. BACKGROUND

A common problem in the calibration of analytical instruments results when the detector responds to more than one sample component and can thus not be considered fully selective [1, 12, 13]. In GFAAS with background correction this situation is infrequent, yet occurs in a few cases when the non-specific absorption components' magnitude differs between measurement of the total and background absorbances. This means that, in effect, the background corrected absorbance signal contains contributions from both the analyte and some other sample component(s). Analogous situations can be found in other areas of analytical chemistry where the detector responds to more than one sample constituent. The solution to some such situations has been found in relating the information contained in the signal shape (response vs time, wavelength, etc.) to the concentration of each constituent using partial least squares (PLS) modelling [18–23].

As a rule, all sample components giving a response at the detector must be calibrated for (although as with most rules there are exceptions [24, 25]). Most applications of PLS modelling have employed calibration samples with known concentrations and similar matrix compositions to envisaged unknowns. This of course requires the availability of either large numbers of suitable reference materials or of alternative analytical methods with which to determine the concentrations of the analyte species in the samples to be used for calibration purposes. Such requirements cannot always be met, and so the generalised standard addition method (GSAM) [12, 13] was used here for calibration. Detailed treatments of the aforementioned multivariate methods (PLS and the GSAM) may be found in the literature [11–16, 18, 19]. However, a brief introduction to the pertinent features of PLS and GSAM for the present application is appropriate. In what follows, the combination of the GSAM with PLS modelling will be denoted PLS–GSAM to be consistent with the terminology used in the first application of the method [26]. In that work, however, the total response was used which resulted in biased estimates of the determined concentrations as discussed in Ref. [26]. Here, the shape of the response (the absorbance/time profile) is used in a manner similar to that employed in most other applications of PLS modelling to analytical calibration problems [18–23].

3. PLS–GSAM

In GFAAS, each point along the background corrected absorbance/time profile contains information relating to the concentration of each sample species, to which the detector responds, present in the atomiser at each time interval. For the spectral interference of cobalt on the gold 242.8 nm line using continuum source background correction, signals of the form shown in Fig. 1 (a–c) are obtained. There is slight temporal resolution of the two components, since an initial positive signal is obtained (due to gold), which becomes negative (below the baseline) as cobalt is volatilised. The goal of multivariate calibration is then to mathematically extract a more complete resolution of these species. To this end, a calibration set is first created by making multi-component standard additions (in this case of gold and cobalt) to one of the samples. This is the function of the GSAM.

The background corrected absorbance profile of the initial sample is then subtracted from each of the corresponding signals with additions, and these differential responses can be used to form the calibration set, see Fig. 1. (Calibration with such differential responses will be denoted DIFF.PLS–GSAM in what follows). For n samples with additions and m points to characterise each absorbance/time profile, an $n \times m$ tensor of differential responses, ΔR, is obtained. (The term "tensor" [24] is used here instead of matrix to avoid confusion with the sample matrix; the terms are equivalent.) Each of the n rows of ΔR describes an absorbance/time profile and each of the m columns the absorbance at a specific time for the

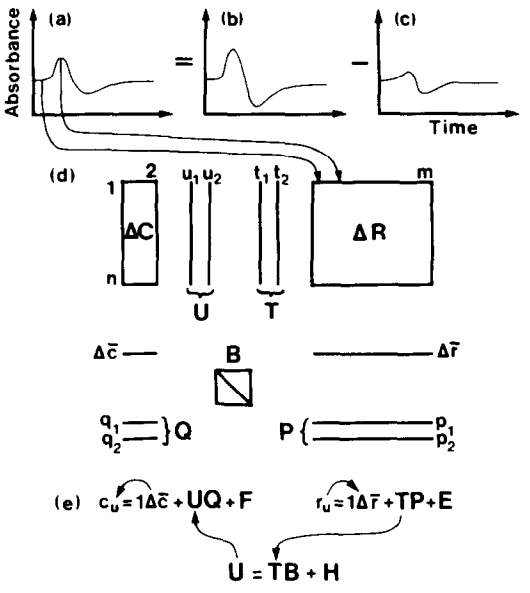

Fig. 1. The PLS calibration model. (a) Standard addition response (gold and cobalt added) is (b) response of sample plus addition minus (c) initial sample response. (d) The responses (absorbance time profiles) are arranged in the block ΔR, which is modelled by the tensors T and P, while U and Q model the standard addition concentrations block ΔC. Subscripts 1 and 2 refer to the first and second PLS components, respectively, and the corresponding vectors. A diagonal tensor B describes the relationship between the blocks, and E, F and H are residual tensors. (e) The response for an unknown sample, r_u, is then used to predict to concentrations of gold and cobalt (c_u).

different standard additions. The corresponding known standard addition concentrations of gold and cobalt are arranged in the $n \times 2$ matrix ΔC.

In making standard additions to one of the samples and subtracting the initial response, the calibration set consists of known concentrations in the sample matrix of interest. Thus, should the matrix alter the signal appearance in any way or interfere in a non-spectral manner, these affects will be modelled by the calibration set. This assumes that the incipient and added sample components are equally affected by the matrix, which is of course the requirement for successful application of the standard addition method in any situation [27]. If this assumption holds true, then the calibration set should be applicable to all samples with the same (or very similar) matrix composition, avoiding the need of having to make multi-component standard additions to all samples.

The aim in PLS is to model each of the tensors or blocks ΔR and ΔC as well as possible while still maintaining maximum correlation between the blocks. This maximises the predictive capabilities of the PLS model [11, 14–16]. First, the mean value of each column in ΔR and ΔC is subtracted from each variable in the column, making subsequent computations well-conditioned [22]. (It should be noted that no variable scaling was used in this work.) Thereafter, two lower dimensional tensors are calculated which model each of the blocks. These lower dimensional tensors are the loadings (P and Q for the blocks ΔR and ΔC, respectively) and the scores (T and U). An inner relation between P and Q is also calculated (diagonal tensor B containing the model regression coefficients [16]), and it is these three, last-named tensors which are used for prediction, as seen in Fig. 1(e). Calculation of the PLS components (two are shown in Fig. 1) is performed by an iterative algorithm [14–16] which extracts the first component to describe the largest amount of variance in the data, the second the greatest part of the remaining variance after the first component, and so on. The iteration continues until no significant variance (information) remains.

It is obviously important to recognise when to stop extracting PLS components from the data, as some of the smaller components will only describe noise in the measurements [11, 14–16, 18–23] and thus not contribute to the predictive power of the model. A means to this end is the method known as cross-validation [28], which, to state the case simply, enables

selection of the optimum number of PLS components to use in the model with respect to prediction.

Cross-validation requires that the calibration set be divided into (typically) four subgroups. Three such groups are then used to compute a PLS component and the concentrations of the left-out group are calculated. The prediction error sum of squares (PRESS) is calculated as Σ (true-predicted concentration)^2 and the omitted group is reinstated, leaving out another group. A new PRESS value is computed and added to the previous one. After all groups have been omitted once only, the total PRESS is divided by the sum of squares of variations around the model before the current PLS component was calculated. This ratio is the cross-validation term, and if less than the threshold value of 0.95 [29], is deemed to have predictive significance. New PLS components continue to be calculated until cross-validation shows that the predictive properties of the model are no longer improved, i.e. the optimum number of components to use in the PLS model has been obtained.

4. EXPERIMENTAL

4.1. *Instrumentation*

A laboratory constructed furnace accomodating integrated contact tubes [30] was mounted on the optical bench of a modified Varian AA-6, as described earlier [31]. This system was equipped with continuum source background correction using a Varian hydrogen hollow cathode lamp. Relevant instrumental parameters are given in Table 1. Absorbance data were acquired at 52.6 Hz using an Ericsson personal computer via a Tecmar Labmaster interface. The GFAAS software was obtained from B. Radziuk (Bodenseewerk Perkin–Elmer, FRG) and permitted storage of background corrected absorbance signals (amongst other functions) as ASCII files.

4.2. *Reagents and materials*

All stock solutions were prepared from reagents of the highest available purity. Gold and cobalt stock solutions were diluted with 1% aqua regia to give the required concentrations immediately prior to commencing the measurements. A matrix modifier, corresponding to 20 μg nickel (as nitrate) on the platform, was added unless as otherwise noted in the relevant text.

Argon of SR-grade was used throughout as the purge gas.

Integrated contact tubes (5.7 mm internal diameter and 19 mm long) were manufactured from single pieces of RW0 quality graphite, and pyrolytically coated (Ringsdorff–Werke GmbH, FRG). Solid pyrolite graphite platforms as supplied by Perkin–Elmer were used.

4.3. *Data analysis by PLS*

A programme was written to convert the ASCII files stored using the GFAAS software to a format suitable for evaluation by PLS using the SIMCA 3B package [29]. An editing programme was also used to perform the following data manipulations: (1) Averaging several absorbance/time profiles; (2) subtraction of initial sample responses from signals obtained following standard additions; (3) data compression.

Background corrected absorbance data were collected from the spectrometer every 19 ms during the 10 s atomisation step using the GFAAS software. This amounts to 526 data points per measurement cycle. Using the experimental design detailed in Table 2, a total of about 1.7×10^4 data points are obtained for a complete GSAM experiment, excluding additional samples. This number of data is too

Table 1. Instrumental parameters for GFAAS measurements

Step	Temp (°C)	Ramp time (s)	Hold time (s)
Ash	600	20	5
Atomise	2200	0	10
Clean-out	2600	1	2

The light source was a Varian gold hollow cathode lamp operated at 6 mA, the wavelength was 242.8 nm and the spectral bandwidth 0.5 nm. Sample volume 10 μl, standard addition volume 10 μl, and modifier volume 5 μl.

Table 2. Experimental design for the determination of gold in cobalt matrices by GFAAS with continuum source background correction using multi-component standard additions and the PLS–GSAM

Addition* ΔAu	ΔCo		
	0	1	2
0	x†	x	x
1	x	x	
2	x		x

* Concentrations in arbitrary units.
† $n=8$, otherwise $n=4$.

large to be handled conveniently by the personal computer, so a reduction in the amount of data was required. Consequently, only the first 350 data points (about 7 s) were used, and further reduction was achieved in two ways: (i) all replicate absorbance profiles were averaged, and these were used to construct the PLS calibration model; (ii) each absorbance profile was compressed by replacing consecutive groups of five data points by the average of each group. Compressed absorbance profiles were then used as the calibration set for PLS modelling.

Both data reduction schemes gave good results, so the second was used as it proved to be more rapid. The total computing time for seven samples (one with six standard additions) is about 45 mins.

4.4. *"Conventional" standard addition methods*

Occasionally, useful determinations have been claimed even when spectral interferences are present [32, 33] or might be expected [34]. In some cases, it is assumed that, at the point of the absorbance maximum, the magnitude of the spectral interference is negligible and calibration can be made using peak height measurements and standard additions [33] or relative to a sample of known composition [34]. For comparison with the PLS–GSAM, results for the determination of gold in cobalt matrices were calculated using the signals where only gold was added. The procedure used is illustrated in Fig. 2.

Using the GFAAS software, it is possible to set integration limits on either side of the peak at the zero absorbance level, so that the area can be calculated over the positive part of the signal (cross-hatched area in Fig. 2(a)). A corresponding peak height value is also obtained, and results calculated in

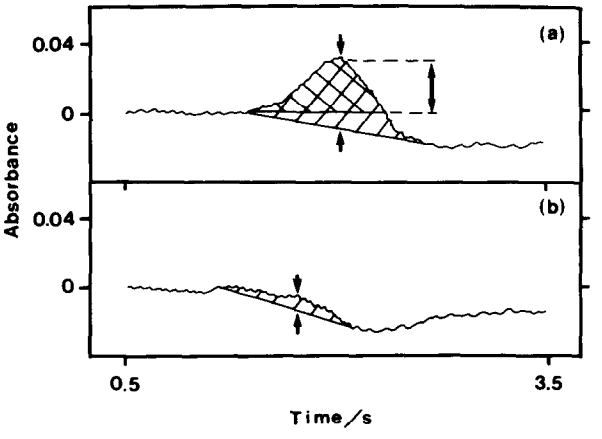

Fig. 2. Illustration of the use of GFAAS software for peak height and area evaluation. Responses for (a) sample 1 containing 10.2 $\mu g l^{-1}$ gold plus 293 $mg l^{-1}$ cobalt and (b) sample 2 containing 2.2 $\mu g l^{-1}$ gold plus 329 $mg l^{-1}$ cobalt. Using standard addition method (SAM) I, integration limits are set at points displaying zero absorbance before and after the peak maximum. The peak height is calculated as given by the double-headed arrow and the area as the cross-hatched region in (a). For sample 2(b), no signal could be obtained, so the gold concentration was evaluated as 0 $\mu g l^{-1}$. For SAM II, integration limits are placed so that a sloping baseline is extrapolated in the interval of interest. The peak height is calculated between the single-headed arrows and the peak area as the hatched region in (a) and (b).

this way are denoted by SAM I (standard addition method). Concentrations based on peak absorbances calculated in this way have been reported by several other workers [33, 34 and references cited therein], less use having been made of peak areas (Ref. [32] is an exception) as these are generally considered to be more susceptible to spectral interferences.

In chromatographic practice, overlapping signals are frequently encountered, and in such cases an artificial baseline extrapolated between points at the extremes of the peak is often used [35]. This method was also evaluated since extrapolation of the baseline can be made using the GFAAS programme. Both peak height and peak area (hatched area in Fig. 2) values can be recovered in this way, and were used to calculate gold concentrations using the standard addition method with extrapolated baselines (SAM II).

It should be noted that the methods described in this section make assumptions concerning the shape of a baseline disturbed by a spectral interference which may not be valid. No such assumptions are necessary in employing the PLS–GSAM.

On a practical note, the time to evaluate results by all but the peak height method without baseline extrapolation is no shorter than that taken for the PLS–GSAM. This is due to the need to tailor integration limits to fit every individual signal and then calculate the concentrations from the resultant data.

5. Results and Discussion

5.1. *Experimental design*

Absorbance/time profiles for a sample containing gold and cobalt before and after multi-component standard additions are shown in Fig. 3. Two features of these signals are worthy of note. First, the initial positive peak resulting from the gold which is volatilised before the cobalt, and second, the negative contribution due to cobalt. In confirmation of results reported elsewhere [8], it was not possible to completely resolve the gold and cobalt signal components by altering the temperature programme.

The traces shown in Fig. 3 can be viewed as linear combinations of over-lapping gold and cobalt signals. To resolve these spectra, standard additions were first made to one sample according to the experimental design given in Table 2. Additions of the two analytes were made both individually and in combination, the latter in order to model interactions between gold and cobalt [36]. It has previously been shown [8] that excess cobalt tends to retard the volatilisation of gold and alter the peak shape. In the present work, however, the presence of 20 μg nickel as matrix modifier probably swamps any effect that varying the amount of cobalt might have on the signal form.

5.2. *Initial results using DIFF.PLS–GSAM*

Results of some initial experiments to determine gold in cobalt matrices by GFAAS with DIFF.PLS–GSAM calibration are summarised in Table 3. Reasonable agreement between the true and predicted gold concentrations is evident, but the results for cobalt are most disappointing. While the major objective of the exercise was to resolve the spectral interference and accurately determine gold, it might be preferable in some situations to obtain good predictions for the interfering species as well. To this end, the underlying reason

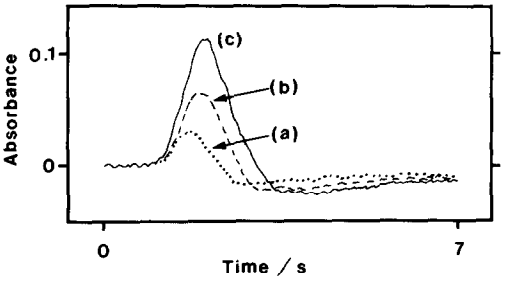

Fig. 3. Absorbance signals for (a) sample 1 (containing 10.2 $\mu g l^{-1}$ gold plus 293 $mg l^{-1}$ cobalt) without and (b, c) with additions. Addition concentrations were (b) 15 $\mu g l^{-1}$ gold and 200 $mg l^{-1}$ cobalt, and (c) 30 $\mu g l^{-1}$ gold and 400 $mg l^{-1}$ cobalt.

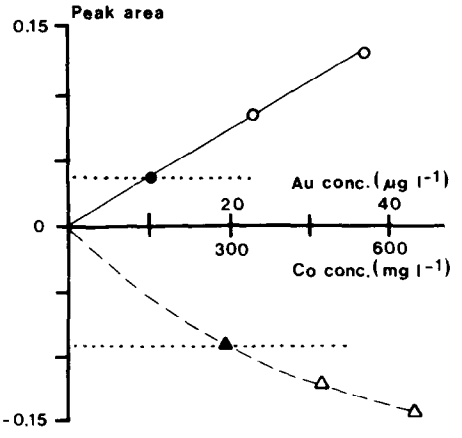

Fig. 4. Background corrected peak areas at the 242.8 nm line with increasing concentrations of gold only (○) or cobalt only (Δ). Filled symbols are equivalent to the initial responses and concentrations for sample 1 and the open symbols to the responses and concentrations following standard additions.

for the poor performance of DIFF.PLS–GSAM with respect to the cobalt results was sought (see Fig. 4).

Figure 4 shows the background corrected peak area response as a function of gold and cobalt concentrations. Calibration by the DIFF.PLS–GSAM model requires that the initial responses are subtracted from signals with additions. Thus it is implicity assumed that the slope of the response function is constant throughout the range of interest (a usual assumption for the standard addition method [27]). This is not the case for cobalt as seen in Fig. 4, and so one of the assumptions made in applying the DIFF.PLS–GSAM model is violated and calibration in this way is destined to give high biased results (Table 3).

5.3. *Modified calibration model*

In an attempt to avoid this problem, a new PLS model was calculated from the same data, this time without subtracting the initial sample response from the signals with additions. Four of the signals without standard additions (see Table 2) were used as unknowns and not included in the calibration set. The ΔR tensor (of differential responses) shown in Fig. 1 and discussed in section 3 was replaced by R (total responses), and n was augmented by one to include the initial sample response. Similarly, a tensor C containing the total concentrations (initial plus added) of gold and cobalt in the samples with and without additions was substituted for ΔC. This new model, which will be referred to as TOT.PLS–GSAM, was used

Table 3. Concentrations of gold in cobalt matrices as determined by GFAAS with continuum source background correction at the 242.8 nm wavelength using DIFF.PLS–GSAM

Sample no.	Au concn. ($\mu g l^{-1}$)		Co concn. ($mg l^{-1}$)	
	True	Pred.	True	Pred.
1	10 2	11.1	293	509
2	2.2	2.1	329	514
3	18.4	22.3	147	433

Standard additions were made to sample 1 (experimental design shown in Table 2) and the response changes were used to construct the calibration set which was then employed to evaluate gold (and cobalt) concentrations in all samples. Twenty micrograms nickel was added to all samples as matrix modifier. A four component PLS model was used which explained 95.7% and 88.1% of the variances in the concentration and response calibration tensors, respectively, and initial sample responses were subtracted from signals with additions.

to re-evaluate the concentrations of gold and cobalt in the samples listed in Table 3, plus some additional "unknowns", and the results are reported in Table 4.

While the modified model, TOT.PLS–GSAM, gives much better results for cobalt, there is apparently some depreciation in the quality of those for gold. This is probably a random event, since the gold concentration in sample 2 is in the region of the detection limit (1 $\mu g l^{-1}$ on a 3σ-basis for a 10 μl sample in the absence of spectral interferences). A disadvantage of the TOT.PLS–GSAM model may lie in the need to have a sample of known composition for calibration purposes. Otherwise, the better predictions for cobalt compared to DIFF.PLS–GSAM are one favourable feature. The good results for cobalt in Table 4, despite considerable curvature in the response function (Fig. 4), also demonstrate the efficacy of PLS in handling slight non-linearities in the data, as has been discussed elsewhere [21].

Samples 4 and 5 in Table 4 were also determined using the TOT.PLS–GSAM model based on standard additions made to sample 1. Additional GFAAS measurements were made using reduced modifier masses of 0 and 5 μg nickel, and typical absorbance signals are shown in Fig. 5. The point of these experiments was to test the ability of the TOT.PLS–GSAM model to recognise signals which have a different shape from those in the calibration set. Such discrimination is achieved by assessing how closely the unknown response resembles the signals for the calibration samples. After fitting the new response to the model, the standard deviation (SD) of the residual (part of the signal not fitted) is calculated, S_{unk}, and compared to the residual SD of the calibration set, S_{cal}. In Table 4, the dissimilarity factor is equal to (S_{unk}/S_{cal}), and for values greater than two, the PLS predictions may be unreliable [29] and should thus be viewed with caution.

The highest dissimilarity factor is obtained for sample 4 (containing only gold) without a modifier, and it can be seen in Fig. 5 that the signal shape for this sample is radically different from the others. Figure 5 also shows that cobalt present in the sample alters the shape of the gold response [8] in a fashion similar to the nickel modifier. The dissimilarity factor is thus a useful feature of PLS, since samples deviating significantly from the calibration model are identified.

Table 4 shows that even the modified TOT.PLS–GSAM model gives poor results for cobalt in sample 4, irrespective of the modifier mass used. There are two factors which may contribute to this. First, cobalt was present at a large concentration in sample 1, to which standard additions were made to form the calibration set. Thus sample 4 containing no cobalt lies outside the range calibrated for. It is well-known that extensive extrapolation of

Table 4. Determination of gold in cobalt matrices by GFAAS using TOT.PLS–GSAM

Sample no.	Au concn. ($\mu g l^{-1}$)		Co concn. ($mg l^{-1}$)		Modifier mass (μg Ni)	Dissimilarity* factor
	True	Pred.	True	Pred.		
1	10.2	10.1	293	295	20	1.11
2	2.2	1.1	329	292	20	1.11
3	18.4	21.7	147	163	20	1.96
4	13.6	15.6	0	119	20	1.90
5	7.4	3.5	180	125	20	1.46
6	0	0.1	183	207	20	1.02
7	27.4	27.3	368	345	20	1.26
4	13.6	18.3	0	348	5	1.56
5	7.4	6.7	180	139	5	1.57
4	13.6	5.6	0	228	0	5.88
5	7.4	9.6	180	266	0	1.63

* See text for definition.

Standard additions were made to sample 1 and total responses and total concentrations (initial plus added) were used to construct the calibration set which was then employed to evaluate the gold and cobalt concentrations. Four additional measurements of sample 1 (not used in the calibration set) were used to provide the values shown. A four component PLS model was used. This explained 93.1% and 87.9% of the variances in the concentration and response tensors, respectively.

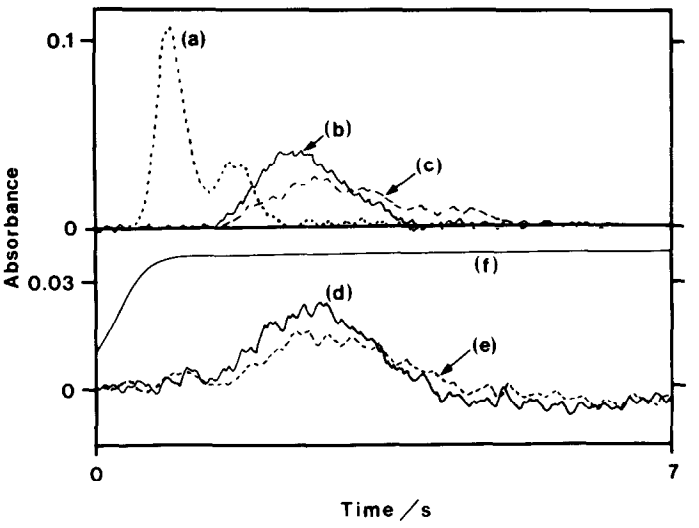

Fig. 5. Effect of nickel matrix modifier on signals for sample 4 containing 13.6 $\mu g l^{-1}$ gold only (upper panel) and sample 5 containing 7.4 $\mu g l^{-1}$ gold plus 180 $mg l^{-1}$ cobalt (lower panel). Modifier mass: (a, d) 0 μg; (b, e) 5 μg; (c) 20 μg. The signal for sample 5 with 20 μg nickel added has been omitted for clarity. Trace (f) is the integrated contact tube temperature profile.

any model outside the region for which it was calibrated may lead to very uncertain results. Second, the aforementioned non-linearity of the cobalt response will magnify any extrapolation errors. The results for cobalt in sample 4 are not, therefore, unexpected and emphasise the need to critically examine the validity of the calibration model.

5.4. *Comparison with "conventional" standard addition approaches*

Finally, we will compare the performance of the TOT.PLS–GSAM model with conventional (i.e. one component) standard addition methods. The results are shown in Table 5 together with two figures of merit for the gold values obtaind by each of the five approaches. It is seen that the TOT.PLS–GSAM gives the lowest bias and standard error of prediction (SEP). The positive bias for both methods based on peak height measurements probably results from curvature of the calibration function, one of the many reasons why peak areas

Table 5. Comparison of results for the determination of gold in cobalt matrices between TOT.PLS–GSAM and standard addition methods (the latter defined in Fig. 2 and section 4.4). The matrix modifier, 20 μg nickel, was used in all cases. Cobalt concentrations in the samples are listed in Table 4

	Au concentration ($\mu g l^{-1}$)					
			SAM I		SAM II	
Sample no.	True	PLS–GSAM	Height	Area	Height	Area
1	10.2	10.1	8.7	5.8	11.4	8.5
2	2.2	1.1	0	0	2.5	1.8
3	18.4	21.7	22.3	16.4	24.3	18.0
4	13.6	15.6	16.0	14.5	15.8	13.2
5	7.4	3.5	8.6	4.7	10.1	7.9
6	0	0.1	2.5	0.6	3.2	1.7
7	27.4	27.3	30.2	26.8	31.6	16.6
	Bias*	+0.03	+ 1.1	−1.3	+2.5	−1.4
	SEP†	2.0	2.3	2.2	3.1	3.9

* Bias is given by $[\Sigma (C_{true}-C_{pred})/n]$.

† Standard error of prediction given by $[\Sigma(C_{true}-C_{pred})^2/n]^{1/2}$.

are generally preferred for quantitative analyses by GFAAS [3] in the absence of spectral interferences. Negative bias for the peak area results is possibly due to failure to adequately approximate the shape of the baseline under the gold peak (see Fig. 2). In any case, the results by any of the SAM variations (section 4.4) are less reliable than those for the PLS–GSAM, as shown in Table 5.

6. Concluding Remarks

The use of PLS–GSAM allows the resolution of and correction for spectral interferences in GFAAS, at least in this application. When the response to one constituent is non-linear, the DIFF.PLS–GSAM gives biased results for that constituent. However, the results for the other component will be satisfactory provided that a linear response is obtained. A slightly modified version, the TOT.PLS–GSAM, can overcome the problem with a non-linear response, but requires that a sample of known composition is available.

An attractive feature of PLS modelling is that unusual samples are identified by the dissimilarity of their responses to the calibration set. This will warn the user that the analyte concentrations cannot be reliably predicted.

The PLS–GSAM model requires that the signal shape can be reproduced, which was possible in this work, but maybe a more difficult condition to fulfil when the spectral interference results from some molecular species. Difficulties may also be envisaged in attempting to make standard additions of a molecular species to the sample. Thus further work is required to evaluate the extent to which the PLS–GSAM can be applied.

One interesting possibility is to use the PLS–GSAM calibration model to predict the concentrations of both the analyte and the spectrally interfering constituent(s). Investigations of this and other characteristics of PLS–GSAM calibration are now under way.

Acknowledgements—We would like to thank W. Lindberg, National Swedish Laboratory for Agricultural Chemistry, Umeå, Sweden, who originally suggested the possibility of using multivariate methods to resolve spectral interferences in GFAAS, B. Hutsch, Ringsdorff–Werke, Bonn, FRG, for supplying us with integrated contact tubes, and I. Berglund and I. Lukkari, University of Umeå, Sweden, for helpful discussions. This work was supported by the Swedish Centre for Environmental Research.

References

[1] H. Kaiser, *Spectrochim. Acta* **33B**, 551 (1978).
[2] A. Walsh, *Spectrochim. Acta* **35B**, 639 (1980).
[3] B. Welz, *Atomic Absorption Spectrometry*, 2nd Edn, VCH, Weinheim (1985).
[4] W. Slavin and G. R. Carnrick, *CRC Crit. Rev. Anal. Chem.* **19**, 95 (1988).
[5] S. R. Koirtyohann and E. E. Pickett, *Anal. Chem.* **37**, 601 (1965).
[6] S. B. Smith and G. M. Hieftje, *Appl. Spectrosc.* **37**, 419 (1983).
[7] T. Hadeishi and R. D. McLaughlin, *Science* **174**, 404 (1971).
[8] G. Wibetoe and F. J. Langmyhr, *Anal. Chim. Acta* **176**, 33 (1985).
[9] R. Wennrich, W. Frech and E. Lundberg, *Spectrochim. Acta* **44B**, 239 (1989).
[10] K. E. A. Ohlsson and W. Frech, *J. Anal. Atom. Spectrom.* **4**, 379 (1989).
[11] S. Wold, C. Albano, W. J. Dunn III, U. Edlund, K. Esbensen, P. Geladi, S. Hellberg, E. Johansson, W. Lindberg and M. Sjöström. In *Chemometrics: Mathematics and Statistics in Chemistry*, (Ed. B. R. Kowalski), Reidel, Dordrecht (1984).
[12] B. E. H. Saxberg and B. R. Kowalski, *Anal. Chem.* **51**, 1031 (1979).
[13] C. Jochum, P. Jochum and B. R. Kowalski, *Anal. Chem.* **53**, 85 (1981).
[14] H. Wold, In *Systems under Indirect Observation*, (Eds. K. Jöreskog and H. Wold), North-Holland, Amsterdam (1982).
[15] S. Wold, A. Ruhe, H. Wold and W. J. Dunn III, *SIAM J. Sci. Statist. Comput.* **5**, 735 (1984).
[16] P. Geladi and B. R. Kowalski, *Anal. Chim. Acta* **185**, 1 (1986).
[17] F. J. Fernandez and R. Giddings, *At. Spectrosc.* **3**, 61 (1982).
[18] W. Lindberg, J-Å. Persson and S. Wold, *Anal. Chem.* **55**, 643 (1983).
[19] H. Martens, Doctoral Thesis, Technical University of Norway, Trondheim (1985).
[20] W. Lindberg, J. Öhman, S. Wold and H. Martens, *Anal. Chim. Acta* **174**, 41 (1985).
[21] M. Otto and W. Wegscheider, *Anal. Chem.* **57**, 63 (1985).
[22] W. Lindberg and B. R. Kowalski, *Anal. Chim. Acta* **206**, 125 (1988).
[23] I. Lukkari and W. Lindberg, *Anal. Chim. Acta* **211**, 1 (1988).
[24] E. Sanchez and B. R. Kowalski, *J. Chemometrics* **2**, 265 (1988).

[25] J. Öhman, P. Geladi and S. Wold, *J. Chemometrics*, submitted for publication.
[26] I. E. Frank, J. H. Kalivas and B. R. Kowalski, *Anal. Chem.* **55**, 1800 (1983).
[27] B. Welz, *Fresenius Z. Anal. Chem.* **325**, 95 (1986).
[28] S. Wold, *Technometrics* **29**, 397 (1978).
[29] S. Wold, *SIMCA-3B Users Manual with Examples*, Chemometrics Group, Department of Organic Chemistry, University of Umeå (1983).
[30] W. Frech, D. C. Baxter and B. Hütsch, *Anal. Chem.* **58**, 1973 (1986).
[31] E. Lundberg and W. Frech, *Anal. Chem.* **53**, 1437 (1981).
[32] K. Saeed, *J. Anal. Atom Spectrom.* **2**, 151 (1987).
[33] B. Sampson, *J. Anal. Atom. Spectrom.* **2**, 447 (1987).
[34] B. E. Jacobson and G. Locklitch, *Clin. Chem.* **34**, 709 (1988).
[35] A. N. Papas, *CRC Crit. Rev. Anal. Chem.* **20**, 359 (1989).
[36] J. C. Miller and J. N. Miller, *Statistics for Analytical Chemistry*, 2nd Edn, Ellis Horwood, Chichester (1988).